Dielectric and Magnetic Behavior of Polycrystalline Copper Doped Holmium Orthoferrite

Fumiya Tsunawaki, Mitsuhiro Matsuo, Hirokazu Shimooka, and Shigemi Kohiki

Department of Materials Science, Kyushu Institute of Technology, Kitakyushu 804-8550, Japan

Polycrystalline $HoFe_{1-x}Cu_xO_3$ sample with x = 0, 0.01, 0.05, and 0.1 exhibited dielectric dispersion at 350, 225, 115, and 110 ^oC with the frequency of 100 kHz, respectively. The spin-reorientation temperature of the sample with x = 0.1 was higher by 2 K than that with x = 0. Substitution of Cu for Fe brought about lowering of the dielectric dispersion temperature and rising of the spin-reorientation temperature.

Recent discovery of the ferroelectric state below ≈330 K of $LuFe_2O_4$ by Ikeda et al.[1] recalled interests in dielectric properties of the rare-earth orthoferrites $RFeO_3$ (R: rare-earth element). The $LuFe_2O_4$ demonstrated dielectric dispersion around the magnetic ordering temperature ≈240 K.[1] The dielectric characteristic temperature of the $LuFe_2O_4$ is rather low for the material utilizable for practical magnetoelectric devices. While there are many studies on the magnetic properties of the $RFeO_3$,[2,3] there are hardly the reports on dielectric properties. The $RFeO_3$ is known to crystallize in an orthorhombically distorted perovskite structure with space group *Pbnm*,[4] and to exhibit weakferromagnetism *WFM* above room temperature *RT*. The $RFeO_3$ becomes a promising material with temperature-margins sufficient for practical device applications if it exhibits the dielectric dispersion around the Néel temperature T_N. T_N of the holmium orthoferrite $HoFeO_3$ is known to be ≈640 K.[5,6] As a first step to explore a new multifunctional material for practical applications, the dielectric and magnetic behavior of $HoFe_{1-x}Cu_xO_3$ was examined in this study.

In the orthorhombic unit cell of $RFeO_3$ the Fe atom is octahedrally coordinated by six oxygen atoms, and the R atoms are located in the large cavities formed by corner-linked FeO_6 octahedra. One of the oxygen atoms forms the common apex of the two adjacent octahedra, consequently each Fe atom is coupled to six Fe nearest neighbors through the superexchange Fe-O-Fe bond. Since the symmetry of the unit cell is low, the alignment of Fe^{3+} spin moments is not strictly antiparallel. Slightly canted Fe^{3+} spin moments give rise to a small net magnetization exhibiting *WFM* below T_N. At *RT* the direction of Fe-sublattice magnetization lies along the *a*-axis, thus a weakferromagnetic moment M_{WFM} appears along the *c*-axis. In the field of Fe-sublattice, there is also a contribution due to the paramagnetic susceptibility of the R^{3+} ions. At the spin-reorientation temperature T_R the direction of the net magnetic moment rotates continuously from the *c*-axis to *a*-axis.[7-11] The $HoFeO_3$ undergoes spin-reorientation transition at ≈50 - 60 K.[12,13]

Substitution of Cu for Fe decreases M_{WFM} of the $HoFeO_3$ because the free ion magnetic moment of Cu^{2+} (1.9 μ_B) is smaller

than that of Fe^{3+} (5.9 μ_B). Since the Ho-sublattice magnetization remains at a constant, an increase of x is considered to lower T_N and to raise T_R for the $HoFe_{1-x}Cu_xO_3$. When the dielectric dispersion occurs around T_N of the $HoFeO_3$, the $HoFe_{1-x}Cu_xO_3$ is expected to demonstrate lowering of the dielectric dispersion temperature T_{disp}, and simultaneously rising of T_R. Here we report presence of the dielectric dispersion around T_N of the $HoFeO_3$ (≈365 °C) for the sample with x = 0, and lowering of T_{disp} with x from 350 °C (x = 0) to 110 °C (x = 0.1) at the frequency f = 100 kHz, and simultaneous rising of T_R by 2 K with the increase of x from 0 to 0.1.

The $HoFe_{1-x}Cu_xO_3$ samples were synthesized by calcination of the mixtures of Ho_2O_3, α-Fe_2O_3 and CuO powders. The Ho_2O_3 (purity >99.9%), α-Fe_2O_3 (purity >99.9%) and CuO (purity >98%) reagents were weighed out with the molar ratio of Ho : Fe : Cu = 1 : 1□x : x (x = 0, 0.01, 0.05, and 0.1), and then mixed in grinding. The mixture was heated at 1000 °C for 12 h in flowing oxygen gas. The powders were reground and heated a few times. As shown in the upper panel of Fig. 1, x-ray diffraction peaks for the samples were attributable to the orthorhombic perovskite structure. The lattice constants of the sample with x = 0 (a = 5.282, b = 5.592 and c = 7.607 Å) were in agreement with those reported (a = 5.282, b = 5.592 and c = 7.608 Å).[14] As shown by the lower panel of Fig. 1, the lattice constants of the orthorhombic unit cell, especially those along the a- and c-axes, increased with x. Such increase of the lattice constants is expected to accompany with an elongation of the superexchange Fe-O-Fe bond, and then to lessen the cant angle θ of the Fe-sublattice magnetization relative to the a-axis. Judging from the ionic radii of Fe^{3+} (0.65 Å), Cu^{2+} (0.73 Å) and Ho^{3+} (0.90 Å), the Cu^{2+} substituted for the Fe^{3+} of the $HoFeO_3$ lattice. Smaller θ and/or smaller M_{WFM} by the substitution would give rise to lowering of T_N and rising of T_R.

As shown in Fig. 2, all the samples exhibited characteristic frequency dispersion in temperature dependence of the dielectric constant ε'. It is known that such dielectric relaxation phenomena are resulted from nano-scale polar-regions presented in the order–disorder type of ferroelectric materials, where motion of the ferroelectric domain boundary gives rise to the dispersion. The substitution is considered to bring about disorder in the arrangement of ion valence on the crystallographically equivalent Fe sites. The electric polarization with mesoscopic order in the $HoFeO_3$ was affected by statistical compositional fluctuation. The sample with x = 0 exhibited the dielectric dispersion around T_N (≈365 °C) of $HoFeO_3$. T_{disp} at f = 100 kHz of the samples with x = 0, 0.01, 0.05, and 0.1 were 350, 225, 115, and 110 °C, respectively. An increase of x lowered T_{disp} rather rapidly, but ε' decreased linearly from 45 (x = 0) to 24 (x = 0.1). The Debye curves for dielectric dispersion ε' and absorption ε'' are symmetric about ωτ = 1. The midpoint of ε' curve and the maximum of ε'' curve occur at a frequency of $\omega_{max} = 1/\tau$. At a given temperature T_p, such a characteristic response frequency was found at a peak in the frequency variation of ε''. The value of the relative variation of T_p per decade of f, $(\Delta T_p/T_p)/\Delta(\log_{10} f)$, for the samples with x = 0, 0.01, 0.05 and 0.1 were 0.37, 0.22, 0.38, and 0.34, respectively. They place the samples in the range of non-interacting fine particles.[15] It is well known that the frequency dependence of T_p obeys an Arrhenius relation: $f = f_0 \exp(-E_a/k_B T)$ where f is the measured frequency, $k_B T$ is the thermal energy, f_0 is a prefactor usually thought of as an attempt frequency, and E_a is the activation energy for polarization fluctuation of each polar-region. When we assume $f_0 = 3\times10^{11}$ Hz, the values of E_a for the samples with x = 0, 0.01, 0.05 and 0.1

are estimated to 0.95, 0.73, 0.57, and 0.55 eV, respectively. E_a decreased rather rapidly with x, as well as T_{disp}.

Field dependent magnetization of the samples with x = 0 and 0.1 measured at 300 K are shown in the upper panel of Fig. 3. The sample with x = 0 demonstrated a sharp increase of magnetization with increasing the applied field H below H = 0.05 T, and a linear field dependence of magnetization above H = 0.05 T. The sample with x = 0.1 showed only the linear field dependence of magnetization. Such field dependences of magnetization were resulted from *WFM* based on the superexchange Fe-O-Fe bond. Extrapolation of a line fitted to the linear portion of the *M-H* curve intersects at a point of $M = M_{WFM}$ and of $H = H_i$. H_i is the internal field acting on the Ho sites.[16] M_{WFM} and H_i amounted to ≈0.01 μ_B/Fe and ≈−0.1 T, respectively. H_i is antiparallel to H. An enhancement of the antiferromagnetic coupling for the sample with x = 0.1 is apparent, as shown in the lower panel of Fig. 3. The sample with x = 0 indicated *WFM* above ≈180 K, antiferromagnetism at ≈180-70 K with the Weiss temperature $\Theta \approx$ –100 K, spin-reorientation at ≈70-50 K, and paramagnetism below ≈50 K. A possible origin of the change at ≈180 K is crossover of the anisotropy contribution. The sample with x = 0.1 demonstrated antiferromagnetic behavior at the temperature ranging from ≈300 K to ≈70 K with $\Theta \approx$ –300 K. Remarkable decease of M_{WFM} by the substitution is also indicated by the inset. The enlarged zero-field-cooled (*ZFC*) magnetization around T_R showed the peak-top shift of +2 K by the substitution. This is considered to be due to the smaller magnetic moment of the Cu^{2+} and/or a decrease of θ for antiferromagnetically coupled spin moments. Such T_R shift by the substitution was reconfirmed by employing the thermoremanence *TMR* which determines the phase transition temperatures of polycrystalline samples.[17] Considerable difference between the field-cooled (*FC*) and *ZFC* magnetization appeared below 70 K (not shown). The temperature of the *TMR* curve falls down to a background level were 60 K and 63 K for the sample with x = 0 and 0.1, respectively. The substitution raised T_R as it was expected.

The $HoFe_{1-x}Cu_xO_3$ samples were highly resistive at 300 K. The order of the *ac* resistivity stayed at 10^6 Ωcm at f = 100 kHz even when Cu^{2+} substituted for Fe^{3+}. The upper panel of Fig. 4 shows an enlargement of the optical absorption ranging from 1.5 to 2 eV with x. As shown by the difference spectra in Fig. 4, especially the absorption peaked at 1.5 eV grew rapidly with x. In the octahedral crystal field, the five-fold-degenerated 3*d*-orbital splits into three-fold t_{2g} and two-fold e_g orbitals. These states line up $t_{2g\uparrow}$, $e_{g\uparrow}$, $t_{2g\downarrow}$, and $e_{g\downarrow}$ with increasing the energy, where ↑ and ↓represent the up-spin and down-spin states, respectively. The electronic configuration for Fe^{3+} in the high-spin state is $t^3_{2g\uparrow}$ and $e^2_{g\uparrow}$, and that for Cu^{2+} is $t^3_{2g\uparrow}$, $e^2_{g\uparrow}$, $t^3_{2g\downarrow}$, and $e^1_{g\downarrow}$. Since the $e^1_{g\downarrow}$ state of Cu^{2+} is half-filled, the Fermi level of the Cu substituted samples are considered to align at the middle of the fundamental band gap (the energy difference between the $e^2_{g\uparrow}$ and $t_{2g\downarrow}$ states) of the sample with x = 0. As illustrated in the lower panel of Fig. 4, electron transition between the Cu^{2+} $e^1_{g\downarrow}$ state and the Fe^{3+} $t_{2g\downarrow}$ empty state brings about the optical absorption at the energy below the fundamental absorption energy. Because all the samples are fundamentally highly resistive, electron hopping between the Cu^{2+} $e^1_{g\downarrow}$ state and the Fe^{3+} $t_{2g\downarrow}$ empty state cannot be expected for the $HoFe_{1-x}Cu_xO_3$ samples even when the electron transition corresponds to the experimentally observed absorption peaked at 1.5 eV. The partially filled e_g band is expected to play a key role in the electronic properties of 3*d*-transition metal oxides. The Cu^{2+} substitution for Fe^{3+} would also give rise to generation of Fe^{4+}

with $t^3_{2g\uparrow}$ and $e^1_{g\uparrow}$ to preserve the charge neutrality for the $HoFe_{1-x}Cu_xO_3$. Since the full-filled $e^2_{g\uparrow}$ state of Fe^{3+} and the half-filled $e^1_{g\uparrow}$ state of Fe^{4+} are considered to locate at the same energy level, electron hopping between Fe^{3+} and Fe^{4+} would partially occur in the $HoFe_{1-x}Cu_xO_3$ samples.

The $HoFe_{1-x}Cu_xO_3$ samples exhibited the dielectric dispersion indicating a typical character of order–disorder type ferroelectric materials. T_{disp} of the sample with $x = 0$ was $\approx$350 °C at f = 100 kHz. The substitution of Cu for Fe lowered T_{disp} from 350 °C ($x = 0$) to 110 °C ($x = 0.1$). The increase of x from 0 to 0.1 raised simultaneously T_R by 2 K. The valence fluctuation in the Fe-sublattice played a central role for the dielectric response of $HoFeO_3$.

A part of this work was performed under the inter-university cooperate research program of the Advanced Research Center of Metallic Glasses, Institute for Materials Research, Tohoku University.

1 N. Ikeda, H. Ohsumi, K. Ohwada, K. Ishii, T. Inami, Y. Murakami, K. Kakurai, K. Yoshii, S. Mori, Y. Horibe, H. Kito, *Nature* (*London*) **436** (2005) 1136.
2 Y.S. Didosyan, H. Hauser, H. Wolfmayer, J. Nicolics, P. Fulmek, *Sens. Actuators A* **106** (2003) 168.
3 Y.S. Didosyan, H. Hauser, W. Toriser, *Int. J. Appl. Electron*. **13** (2001) 277.
4 S. Geller, E.A. Wood, *Acta Crystallogr*. **9** (1956) 563.
5 S.C. Parida, S.K. Rakshit, Z. Singh, *J. Solid State Chem*. **181** (2008) 101.
6 M. Eibschutz, S. Shtrikman, D. Treves, *Phys. Rev.* **156** (1967) 562.
7 R.L. White, *J. Appl. Phys*. **40** (1969) 1061.
8 W.C. Koehler, E.O. Eollan, M.K. Wilkinson, *Phys. Rev*. **118** (1960) 58.
9 R.M. Bozorth, V. Kramer, *Coloq. Int. Magn. Grenoble, Suppl. J. Phys. Radium* **20** (1959) 329.
10 I.E. Dzyaloshinski, *J. Phys. Chem. Solids* **4** (1958) 241.
11 T. Moriya, *Phys. Rev.* **120** (1960) 91.
12 K. Saito, A. Sato, A. Bhattacharjee, M. Sorai, *Solid State Commun*. **120** (2001) 129.
13 J. Mareschal, J. Sivardiere, *J. Phys*. (Paris) **30** (1969) 967.
14 JCPDS 46-0115.
15 J.L. Dormann, D. Fiorani, E. Tronc, *Adv. Chem. Phys*. **98** (1997) 283.
16 A.H. Cooke, D.M. Martin, M.R. Wells, *J. Phys. C* **7** (1974) 3133.
17 A. Bombik, B. Lesniewska, A.W. Pacyna, *J. Magn. Magn. Mater.* **214** (2000) 243.

Fig. 1 by K.O/ KIT, JPN

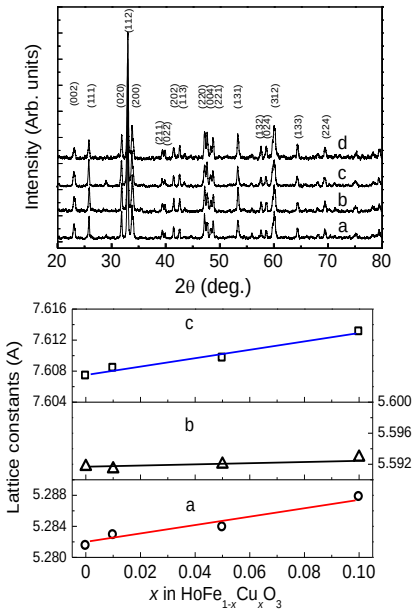

Fig. 1 X-ray diffraction patterns (upper panel) and lattice constants for the orthorhombic unit cell (lower panel) of the samples with x = 0 (a), 0.01 (b), 0.05 (c), and 0.1 (d) measured with a Rigaku CN2013 diffractometer with Cu $K\alpha$ radiation.

Fig. 2 by K.O/ KIT, JPN

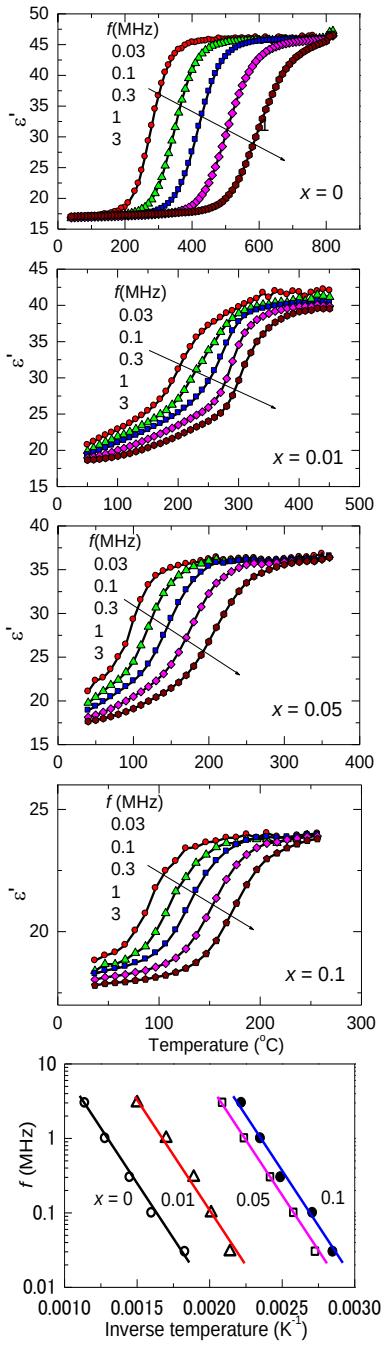

Fig. 2 Dielectric dispersion and temperature variation of the characteristic frequency of the samples with x = 0, 0.01, 0.05, and 0.1 measured with a HP 4291 RF impedance analyzer. The dielectric constant measured at the frequency ranging from 30 kHz to 3 MHz in the external field E = 245 V/cm. The Arrhenius relation is indicated by a solid line for each sample.

Fig. 3 by K.O/ KIT, JPN

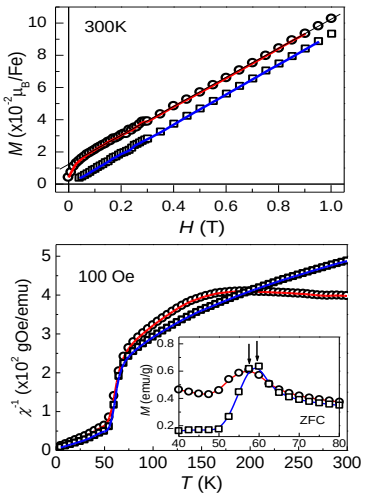

Fig. 3 Initial magnetization curves (upper panel) and temperature dependence of inverse susceptibility (lower panel) of the samples with $x = 0$ (○) and 0.1 (□) measured at 300 K by a Quantum Design MPMS 5S SQUID magnetometer. Inset: enlarged magnetization curves around T_R of the samples cooled in the field of 100 Oe. The arrows indicate the top of the curves.

Fig. 4 by K.O/ KIT, JPN

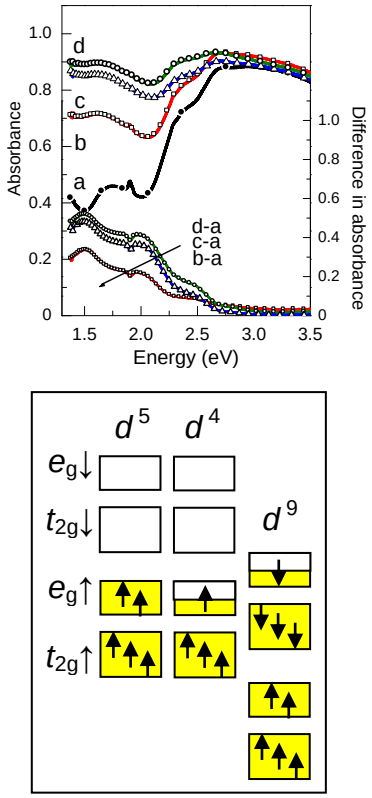

Fig. 4 Upper panel: ultraviolet-visible absorption spectra (the left hand side scale) of the samples with x = 0 (a), 0.01 (b), 0.05 (c), and 0.1 (d) measured with a JASCO V-550 spectrometer. Difference spectra (the right hand side scale) between the samples x = 0.01 and 0 (b – a), x = 0.05 and 0 (c – a), and x = 0.1 and 0 (d – a), are also presented. Lower panel: scheme of the electronic states of Fe^{3+} (d^5), Fe^{4+} (d^4) and Cu^{2+} (d^9) in the octahedral crystal field.